Evaluation of Deuterium Isotope Effects in Normal-Phase LC–MS–MS Separations Using a Molecular Modeling Approach

Sunil S. Iyer[1], Zong-Ping Zhang[1,2], Glen E. Kellogg[3], and **H. Thomas Karnes[1,*]**

[1]Department of Pharmaceutics, School of Pharmacy, Virginia Commonwealth University, Richmond, VA 23298-0533, [2]PPD Development, 2244 Dabney Road, Richmond, VA 23230-3323 and [3]Department of Medicinal Chemistry, School of Pharmacy and Institute for Structural Biology and Drug Discovery, Virginia Commonwealth University, Richmond, VA 23298-0540.

Abstract

Molecular modeling of stationary phases presents a unique challenge because there is little available experimentally derived structural information. Verified interaction mechanisms at a molecular level with analytes are also rare. Molecular mechanics calculations using the Tripos force field were carried out to qualitatively and quantitatively assess stationary phase interactions. Binding energy values of –15.40, 15.28, –12.53, and –12.34 kcal/mol, respectively, are obtained for olanzapine (OLZ), OLZ-D_3, des-methyl olanzapine (DES), and DES-D_8 that corresponded to the retention behavior of the four compounds observed using liquid chromatography–mass spectrometry (MS)–MS. The model explains, semiquantitatively, the deuterium isotope effect in the normal-phase chromatographic separation of these compounds.

Introduction

Careful assessment of matrix effects constitutes an integral and important part of validation of any quantitative liquid chromatography (LC)–mass spectrometry (MS)–MS method utilized in support of pharmacokinetic studies (1). Despite years of study, the mechanism and the origin of matrix effects are still not fully understood. Various methods that are used to minimize or eliminate matrix effects include modifying the retention factor (k), using stable isotope-labeled analogs as internal standards, improving sample extraction procedures, and evaluating different ionization mechanisms. Use of stable isotope-labeled analogs as internal standards has been highly recommended because matrix effects should not affect the relative efficiency of ionization of the drug and its stable isotope-labeled internal standard (2). However, an earlier study in our laboratory (3) showed that matrix effects persisted in a reversed-phase LC–MS–MS method for the analysis of olanzapine (OLZ) des-methyl olanzapine (DES) and its metabolite, although deuterated internal standards had been used. The persistence of matrix effects may have been attributable in part to a slight separation ($R_s < 0.16$ for both analytes) of the analyte and its deuterated internal standard in the reversed-phase mode. This apparent isotope effect was thought to be attributable in part to a slight separation of the isotopes caused by adsorption mechanisms and suggests that changes in the properties of the analytes upon deuteration occur such that matrix effects are not fully compensated for. A separation of the analytes from their respective deuterated internal standards was achieved using normal-phase LC to further investigate this. Normal-phase separation was employed to achieve a more significant separation to facilitate evaluation of the molecular modeling approach.

The International Union of Pure and Applied Chemistry defines kinetic deuterium isotope effects as "changes in the reaction rates of molecules when one or more of its hydrogens has been replaced by deuterium" (4). This could also be viewed in the context of a difference in the interaction behavior of the analytes upon deuteration. Wade (5) reviewed isotope effects on noncovalent interactions between biological and other molecules, as well as changes in the physical properties of a molecule that are a consequence of deuteration, such as changes in polarity, polarizability, and molecular volume. The article suggests that the physical basis of secondary kinetic isotope effects, in which there is a change in the overall reaction rate without cleavage of the covalent bond to the isotopic atom, is the difference in the lengths of the C–D and C–H bonds. The slightly shorter length of the C–D versus the C–H bond results in a slightly increased ability to donate electron density via an inductive effect, and the reduced amplitude of C–D bending vibrations, versus those of C–H, results in a smaller size of the group of atoms containing D. A few contradictory applications in chromatography (6–8) point out that the replacement of carbon-bound hydrogen with deuterium makes a molecule less polar in most cases. This has been termed the "inverse isotope effect", and the opposite effect has also been reported in which deuterium substitution resulted in an increase in polarity of the compound. In the former case, deuteration of

* Author to whom correspondence should be addressed: email tom.karnes@vcu.edu.

the C–H groups was accompanied by a small increase in the lipophilicity of isotopomers. This inverse isotope effect was not affected by the polarity of the stationary phase (9). In the latter case, during reversed-phase high-performance liquid chromatography (HPLC), the deuterated isomer eluted before its nondeuterated counterpart, indicating that there was less interaction between the stationary phase and the deuterated compound than there was between the stationary phase and the nondeuterated compound. It was noted that the IR oscillation frequency of the C–H bond was higher than that of the C–D bond (3300 vs. 2334 cm^{-1}, respectively) and this could induce greater forces of attraction between the bond and the stationary phase. Elution from the column is therefore slowed with respect to the deuterated compound. Thus, a generalization has been made that deuterated molecules may have increased or decreased lipophilicity depending upon the number and position of deuterium substitution with respect to the location of heteroatoms in the molecule.

A paper dedicated to comparative proteomics (10) discusses identification of the structural features responsible for resolution of heavy isotope-coded peptides in reversed-phase chromatography. Bovine serum albumin and cytochrome-c were subjected to proteolysis to yield tryptic peptides. These were derivatized with coding agents that varied in structure, number, and placement of the deuterium atoms. The resolution of the isotopically coded peptides was achieved using a C_{18} column under gradient conditions. A term, "specific resolution", was coined that can be defined as the ratio of chromatographic resolution to the total number of deuterium atoms incorporated into the peptide during derivatization. The authors observed some general trends including (*i*) the probability of a deuterium atom interacting with the stationary phase in the column and impacting resolution is greatly diminished by placing it adjacent to a hydrophilic group, as explained by solvophobic theory, and (*ii*) the isotope effect can be minimized by using smaller numbers of deuterium atoms in the coding agents. None of the aforementioned papers address the mechanistic aspects for the separations.

Atomistic molecular modeling has been successfully implemented in several disciplines to make predictions and to gain new insights. Theoretical studies in molecular recognition involving chiral stationary phases have been described (11–13). Molecular mechanics is a nonquantum mechanical method of computing structures, energies, and some properties of molecules. It models a molecule as if its atoms and bonds are interacting balls and springs, using equations from classical Newtonian physics. Thus, a molecule is viewed as a collection of particles (nuclei) held together by elastic forces (electrons) analogous to springs in simple harmonics. The electrons are thereby treated implicitly, contrasting this tool with quantum mechanics in which electrons are treated explicitly. Classical mechanics employs an empirical force field (EFF), which is a template for reproducing a molecule's potential energy surface. Internal coordinates such as bond lengths, bond angles, and torsion angles define the potential energy functions of any molecule. Empirical force fields describe bond stretching, bond angle bending, and nonbonded interactions. The sum of all these interactions contributes to an amount of strain in the molecule. Once this characterization has been carried out, moving the particles towards their equilibrium positions minimizes the internal energy of the molecule. This is called "energy minimization" or "geometry optimization". The center of each analyte is defined as the origin and position of the analyte with respect to the chiral stationary phase, as defined by a set of spherical polar coordinates, r, θ, and ϕ (14). Among the various types of interactions between molecules, the Van der Waals and electrostatic forces of attraction are worth mentioning at this point. When two molecules approach each other without forming a chemical bond, there is a slight attraction between them because of a mutual distortion of their electron clouds giving rise to a Van der Waals force (15). Dipolar molecules frequently tend to align themselves with their neighbors so that the negative pole of one molecule points towards the positive pole of the next. Thus, large groups of molecules may be associated through weak *dipole–dipole* or Keesom forces. Permanent dipoles are capable of inducing an electric dipole in nonpolar molecules that are easily polarizable, in order to produce *dipole-induced dipole* or Debye interactions. Nonpolar molecules, on the other hand, can induce polarity in one another by *induced dipole-induced dipole*, or London forces of attraction (16). Electrostatic interactions are governed by Coulomb's law and thus decrease inversely with the distance between the two species.

Cheng et. al. (17) attempted to predict the retention behavior of test mixtures of compounds in bonded-phase LC using a molecular dynamics approach. The computational procedure of molecular dynamics generates a trajectory, or a collection of structures, over time, in which each structure has an associated potential or kinetic energy as well as a temperature (13). Simulations for two sets of compounds interacting with the stationary and mobile phases have been described. The interaction energy of stationary phase adsorption and mobile phase solubilization of the analytes were calculated, and an attempt has been made to compare these interaction energies with the experimental orders of retention. However, a few discrepancies exist in the interpretation such that the interaction energies could not be correlated well with the retention order across the two sets of compounds. In addition, no distinction has been made between the mechanisms of interac-

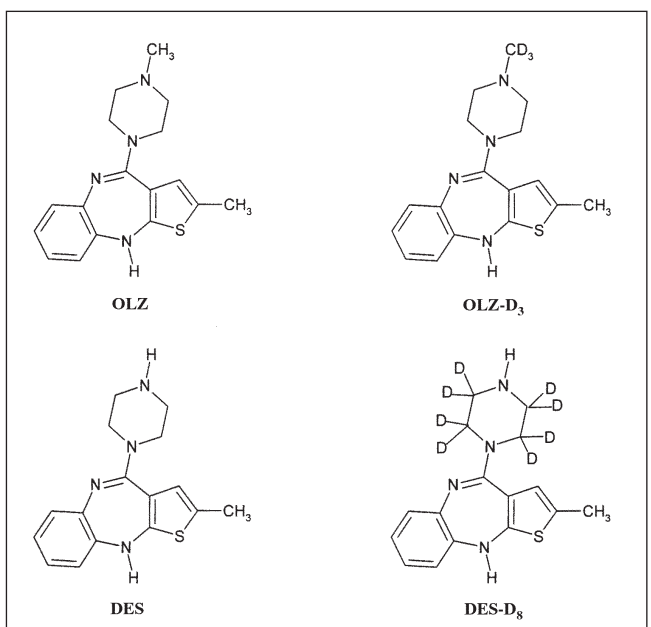

Figure 1. Structures of the analytes.

tion, partitioning, or adsorption of solutes occurring within the column, though thus far such a distinction in reversed-phase chromatography is not apparent from thermodynamic considerations (18).

We have obtained the separation of OLZ, DES, OLZ-D_3, and DES-D_8 (Figure 1) by the use of normal-phase LC and have used a molecular modeling approach to probe the interactions of the four analytes with the modeled stationary phase. This study therefore calculates binding interaction energies at different positions of the analytes with respect to the modeled stationary phase and compares these energies with the experimental separation observed. Our approach, though simple, explains the order of retention of the four compounds on the normal-phase column.

Experimental

LC–MS–MS conditions

OLZ, DES, and their respective deuterated internal standards, viz. OLZ-D_3 and DES-D_8, were provided by PPD Development (Richmond, VA). The LC system consisted of a HP series 1100 pump (Agilent Technologies, Palo Alto, CA) and CTC HTS-PAL autosampler (Leap Technologies, Carrboro, NC). The separation of the analytes from their deuterated internal standards was achieved using a Nucleosil Silica (5 µm, 2 × 50 mm) column procured from Ansys Technologies (Lake Forrest, CA). Mobile phases A and B consisted of 20mM ammonium acetate (pH 9.65) and a 75:25 mix of acetonitrile–methanol, respectively. A linear gradient comprising change of mobile phase A from 5% to 50% over 0.5 min, holding until 2 min, and switching back to 5% mobile phase A was used. The flow rate was constant at 0.4 mL/min. The mass detector was an API 3000 (MDS Sciex, Toronto, Canada) with a turbo ion spray source. Multiple reaction monitoring scanning was employed using the positive ion mode with the transitions 313.2–256.0, 299.0–256.0, 316.1–256.0, and 306.9–213.0, respectively, for OLZ, DES, OLZ-D_3, and DES-D_8.

Modeling stationary phase and analytes

Molecular modeling simulations were performed using SYBYL software version 6.8 (Tripos, St. Louis, MO). The first step consisted of developing a suitable model for the stationary phase. Modeling normal-phase stationary phases presents a significant challenge because few structural details are experimentally available. The surface is composed of different types of silanol groups and siloxanes (19), as represented in Figure 2. Though attempts have been made (20) to quantitate these, little knowledge is available about the relative proportion of the silanols and siloxanes in normal-phase chromatographic columns. For the purpose of modeling, the diamond-like orderly structure exhibiting a 10-atom skeletal cage was chosen as the basic unit (21). In ordinary hydrocarbon chemistry, adamantane exhibits the same 10-atom skeletal cage. Insertion of an oxygen atom between each pair of silicon atoms considerably expands (~ 50%) the Si frame, which creates a cage with a large hole at the center. This openness is a characteristic feature that is important to the ion-exchange and molecular-sieve chromatographic properties of these materials. The valencies of the silicon atoms not bound to other silicon or oxygen atoms in the simulation were satisfied by the addition of hydroxyl groups, thus representing a polar normal-phase chromatographic surface. This was followed by an energy minimization to 0.05 kcal/mol gradient step-size, which yielded a surface of approx. 15 × 25 Å. The Gasteiger-Hückel method for the calculation of atomic charges was employed throughout. This method (22) is a combination of two other methods, the Gasteiger-Marsili method to calculate the σ component of the atomic charge and the Hückel method to calculate the π component of the atomic charge.

For modeling the deuterated analytes (OLZ-D_3 and DES-D_8), the force constant and bond-length parameters defining the C.3 (sp^3 hybridized carbon)–D bond in the Tripos force field were modified to 800 and 1.075 Å, respectively, as opposed to 662.4 and 1.100 Å for the C.3–H bond. The four analytes were then drawn and the energy minimized. Each analyte was rolled over the stationary phase surface and a 3-D visual examination was conducted to qualitatively assess the likelihood of analyte–stationary phase interactions. Twenty-two models were created in such a manner. Bond length constraints were applied for some positions of hydrogen bonds but were removed prior to the energy minimization step. This was again followed by energy minimization of the resulting complexes to 0.05 kcal/mol gradient step-size. Finally, energy calculations were performed for each position as described in the following section.

Binding energy calculations

Energy calculations used the Tripos force field (23) in SYBYL. The total energy E_{total} for an arbitrary geometry of a molecule derived from a force field is given by the sum of energy contributions. For the Tripos force field, this can be represented as:

$$E_{total} = \Sigma E_{str} + \Sigma E_{bend} + \Sigma E_{oop} + \Sigma E_{tors} + \Sigma E_{vdw} + \Sigma E_{elec} + \Sigma E_{constraints} \quad \text{Eq. 1}$$

where the sums extend all over the bonds, bond angles, torsion angles, and nonbonded interactions between atoms not bound to each other or to a common atom; E_{str} is the bond stretching energy term; E_{bend} is the angle bend energy term; E_{oop} is out of plane bending energy term caused by the bending of bonds from their natural values; E_{tors} is the torsional energy term attributable to the twisting of bonds; E_{vdw} is the Van der Waals energy term arising because of nonbonded interactions; E_{elec} is the electrostatic energy term; and $E_{constraints}$ is an energy term for the artificially inserted constraints (if any).

The Tripos force field treats the hydrogen bonds as nondirectional and electrostatic in nature. To

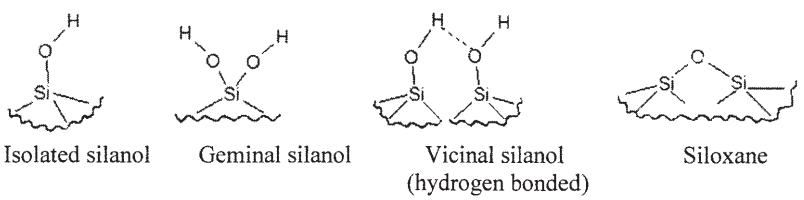

Figure 2. Various types of silanols and siloxane present on the chromatographic surface.

accommodate this, calculations in which hydrogen bonds are expected to be important include partial charges and the electrostatic contributions. Hydrogen bond energies are included in the evaluation of the force field by scaling the Van der Waals interactions between N, O, and F and hydrogens bonded to N, O, or F.

Thus, the binding energy (ΔE) for each position can be calculated as:

$$\Delta E = (E_{analyte} + E_{stationary\ phase}) - (E_{analyte+stationary\ phase}) \qquad \text{Eq. 2}$$

where $E_{analyte}$, $E_{stationary\ phase}$, and $E_{analyte+stationary\ phase}$ represent the total energies of the free unbound analyte, unbound stationary phase and the bound analyte–stationary phase complex, respectively. During the calculation of average binding energy, any molecular model for analyte–stationary phase complexes that exhibited positive ΔE values were omitted from futher consideration because these are not energetically possible.

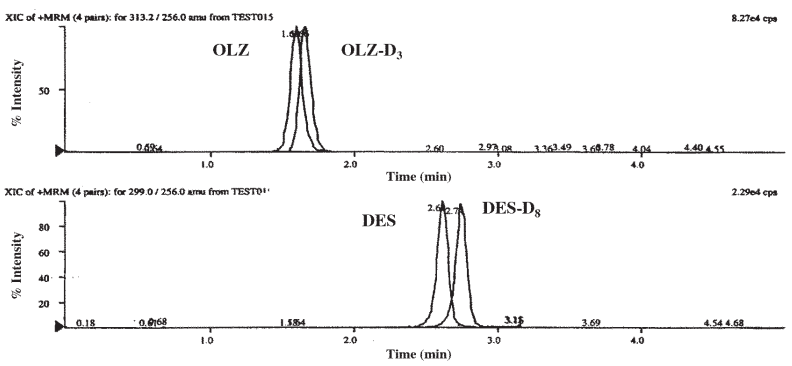

Figure 3. Chromatogram showing the normal-phase LC–MS–MS separation of the four analytes.

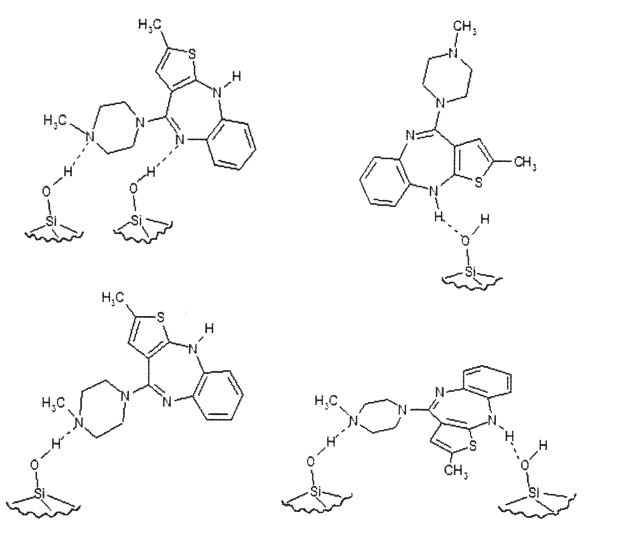

Figure 4. Representative positions of the analyte (OLZ) interacting with the stationary phase through hydrogen bond formation.

Table I. Comparison of Retention Time with the Binding Energy of Each Analyte

Compound	Retention time (min)	Binding energy (kcal/mol)
OLZ	1.60	–15.40
OLZ-D_3	1.66	–15.28
DES	2.62	–12.53
DES-D_8	2.74	–12.34

Results and Discussion

Figure 3 shows the separation obtained using normal-phase HPLC–MS–MS. It is apparent from the chromatogram that the resolution of DES-D_8 (R_s = 0.73) is much better than that of OLZ-D_3 (R_s = 0.34) from their respective nondeuterated analogs. This is in accordance with the observation of earlier workers (10) that increasing the number of deuterium substitutions increases the potential resolution between deuterated and nondeuterated analogs.

The molecular models, created as previously described, were examined qualitatively for analyte–stationary phase interactions upon minimization. There are, in fact, a nearly infinite number of positions at which the analyte may have interactions with the stationary phase. One method of limiting the search, however, is to specify distance constraints between pairs of atoms. Assuming that a set of molecules presents a common range of distances between two particular molecular features that are chemically relevant, the search can be reduced to the exploration of the restricted conformational space defined by the acceptable range for this particular interatomic distance. For a hydrogen bond, this distance is between 1.7 and 2.3 Å. Different models of the bound analyte with the stationary phase revealed a different number and position of the hydrogen bonds. A few representative positions are shown in Figure 4. Out of 22 models created for OLZ and DES, 6 and 8 positions, respectively, showed positive binding energies and were therefore discarded as discussed in the previous section. The mean binding energies of the compounds along with their retention times are shown in Table I. The calculated binding energy of DES was found to be 2.87 kcal/mole greater than that of OLZ and, thus, it would be expected to be retained longer in the column. These calculations are consistent with the retention order that was experimentally observed. Furthermore, it was found that the difference in calculated binding energy between OLZ and OLZ-D_3 was 0.12 kcal/mole and that between DES and DES-D_8 was 0.19 kcal/mole. This explains the larger resolution of the latter pair of isotopologs. Thus, these energies explain the order of retention of the four analytes observed experimentally.

Conclusion

The molecular modeling approach provides a useful semiquantitative tool in the understanding of analyte–stationary phase interactions. Because of a difference in the size of the atoms, the

substitution of hydrogen with deuterium leads to differences in the binding interaction energies of deuterated and nondeuterated analytes bound to the stationary phase. The estimated binding energies explain the order of retention of the four analytes observed experimentally. These are simple models for very complex phenomena; nevertheless, useful information can be obtained. Further investigations are needed to prove if these differences in the interaction energies of compounds upon deuteration could offer a possible explanation for differences in matrix effects observed in LC–MS–MS analyses.

Acknowledgments

The authors thank PPD Development for the LC–MS–MS intrumentation and the VCU Institute of Structural Biology and Drug Discovery, Virginia Biotechnology Research Park (Richmond, VA) for the molecular modeling facilities.

References

1. B.K. Matuszewski, M.L. Constanzer, and C.M. Chavez-Eng. Strategies for the assessment of matrix effect in quantitative bioanalytical methods based on HPLC-MS/MS. *Anal. Chem.* **75:** 3019–30 (2003).
2. C.M. Chavez-Eng, M.L. Constanzer, and B.K. Matuszewski. High-performance liquid chromatographic–tandem mass spectrometric evaluation and determination of stable isotope labeled analogs of rofecoxib in human plasma samples from oral bioavailability studies. *J. Chromatogr. B* **767:** 117–29 (2002).
3. C. Chin, Z.P. Zhang, and H.T. Karnes. A Study of matrix effects on an LC/MS assay for olanzapine and desmethyl olanzapine. *submitted to J. Pharm. Biomed. Anal.* (2002).
4. G.P. Moss. *IUPAC: Recommendations on Organic & Biochemical Nomenclature, Symbols & Terminology.* http://www.chem.qmul.ac.uk/iupac/ (October 20, 2003).
5. D. Wade. Deuterium isotope effects on noncovalent interactions between molecules. *Chem.-Biol Interact.* **117:** 191–217 (1999).
6. A. Bechalany, N. El Tayar, P.A, Carrupt, B. Testa, J.B. Falconnet, Y. Cherrah, Y. Benchekroun, and J.L. Brazier. Isotope effect on the lipophilicity of deuterated caffeines. *Helv. Chin. Acta.* **72:** 472–76 (1989).
7. P.R. Dluzneski and J.W. Jorgenson. New method for the preparation of small diameter columns with polymeric stationary phases for open tubular liquid chromatography. *J. High. Resolut. Chromatogr.* **11:** 332–36 (1988).
8. R. Baweja. Application of reversed-phase high-performance liquid chromatography for the separation of deuterium and hydrogen analogs of aromatic compounds. *Anal. Chim. Acta.* **192:** 345–48 (1987).
9. J. Bermejo, C.G. Blanco, and M.D. Guillén. Gas chromatography of deuterated and protiated chloro derivatives of 1,4-dimethylbenzene. *J. Chromatogr.* **351:** 425–32 (1986).
10. R. Zhang, C.S. Sioma, R.A. Thompson, L. Xiong, and F.E. Regnier. Controlling deuterium isotope effects in comparative proteomics. *Anal. Chem.* **74:** 3662–69 (2002).
11. K. Lipkowitz. Theoretical studies of brush-type chiral stationary phases. *J. Chromatogr. A* **666:** 493–503 (1994).
12. K. Lipkowitz. Theoretical studies of type II-V chiral stationary phases. *J. Chromatogr. A* **694:** 15–37 (1995).
13. W.J. Kowalski, J. Nowak, and M. Konior. Modeling of selected enantioseparation mechanisms in the gas and liquid chromatography with the aid of molecular mechanics. *Anal. Sci.* **17 Suppl.:** i757–60 (2001).
14. K.B. Lipkowitz, B. Baker, and R. Zegarra. Theoretical studies in molecular recognition: Enantioselectivity in chiral chromatography. *J. Comput. Chem.* **10:** 718–32 (1989).
15. E.S. Gould. *Mechanism and Structure in Organic Chemistry*. Holt, Rinehart and Winston, Inc., New York, NY, 1964, pp. 50–53.
16. A. Martin. *Physical Pharmacy*, 4th ed. B.I. Waverly Pvt. Ltd., New Delhi, India, 1994, pp. 22–24.
17. C.Y. Cheng, T.L. Chen, and B.C. Wang. Molecular dynamics simulation of separation mechanisms in bonded phase liquid chromatography. *J. Mol. Struc. (Theochem).* **577:** 81–90 (2002).
18. A. Vailaya and C. Horváth. Retention in reversed-phase chromatography: partition or adsorption? *J. Chromatogr. A* **829:** 1–27 (1998).
19. J.D. Sunseri, W.T. Cooper, and J.G. Dorsey. Reducing residual silanol interactions in reversed-phase liquid chromatography: Thermal treatment of silica before derivatization. *J. Chromatogr. A* **1011:** 23–29 (2003).
20. S. Laufer. Quantitative determination of surface groups of silica: IR-analysis of isolated silanol groups in pyrogenic silica. *J. Mol. Struc.* **60:** 409–14 (1980).
21. K.F. Purcell and J.C. Kotz. *Inorganic chemistry.* W.B. Saunders, Philadelphia, PA, 1977, pp. 317–27.
22. *Force Field Manual ver. 6.6,* chapter 5. Tripos Inc., St. Louis, MO, 1999, p. 164.
23. *Force Field Manual ver. 6.6,* chapter 3. Tripos Inc., St. Louis, MO, 1999, p. 81.

Manuscript accepted July 6, 2004.